Lung Cancer: Targets and Therapy

Dovepress
open access to scientific and medical research

Open Access Full Text Article

REVIEW

Clinical staging of malignant pleural mesothelioma: current perspectives

This article was published in the following Dove Press journal:
Lung Cancer: Targets and Therapy
18 August 2017
Number of times this article has been viewed

Maria Bonomi[1]
Costantino De Filippis[2]
Egesta Lopci[3]
Letizia Gianoncelli[1]
Giovanna Rizzardi[4]
Eleonora Cerchiaro[1]
Luigi Bortolotti[4]
Alessandro Zanello[2]
Giovanni Luca Ceresoli[1]

[1]Department of Oncology, Thoracic and GU Oncology Unit, [2]Department of Radiology, Cliniche Humanitas Gavazzeni, Bergamo, [3]Nuclear Medicine Unit, Humanitas Clinical and Research Hospital, Milan, [4]Department of Thoracic Surgery, Cliniche Humanitas Gavazzeni, Bergamo, Italy

Abstract: Malignant pleural mesothelioma (MPM) is a disease with limited therapeutic options, the management of which is still controversial. Diagnosis is usually made by thoracoscopy, which allows multiple biopsies with histological subtyping and is indicated for staging purposes in surgical candidates. The recommended and recently updated classification for clinical use is the TNM staging system established by the International Mesothelioma Interest Group and the International Association for the Study of Lung Cancer, which is based mainly on surgical and pathological variables, as well as on cross-sectional imaging. Contrast-enhanced computed tomography is the primary imaging procedure. Currently, the most used measurement system for MPM is the modified Response Evaluation Criteria in Solid Tumors (RECIST) method, which is based on unidimensional measurements of tumor thickness perpendicular to the chest wall or mediastinum. Magnetic resonance imaging and functional imaging with ^{18}F-fluoro-2-deoxy-D-glucose positron-emission tomography can provide additional staging information in selected cases, although the usefulness of this method is limited in patients undergoing pleurodesis. Molecular reclassification of MPM and gene expression or miRNA prognostic models have the potential to improve prognostication and patient selection for a proper treatment algorithm; however, they await prospective validation to be introduced in clinical practice.

Keywords: malignant pleural mesothelioma, staging, contrast-enhanced computed tomography, magnetic resonance imaging, positron-emission tomography

Introduction

Malignant pleural mesothelioma (MPM) is a disease with a poor prognosis and limited therapeutic options. After years of clinical research, its management is still controversial. Few large Phase III randomized clinical trials have been conducted to evaluate the efficacy of specific treatments, and data to support clinical practice are often based on small Phase II clinical trials or retrospective data-set analyses.

Difficulties in diagnosing and staging, especially in early disease, have thwarted the development of a generally accepted stage-related approach. Although the initial evaluation of pleural effusion is often made by thoracentesis with cytological assessment, a pleural biopsy is recommended by most guidelines, preferably by thoracoscopy.[1] Thoracoscopy allows good visual examination of the pleural space, affording multiple biopsies and staging definition in patients considered for surgery. An accurate histological subtyping is mandatory as a prognostic factor and to guide therapeutic management, mainly when a multimodality approach is planned.[2]

Early staging systems reflected mainly the experiences of individual institutions on limited data sets not externally validated, with discrepancies resulting in inconsistent

Correspondence: Giovanni Luca Ceresoli
Department of Oncology, Thoracic and GU Oncology Unit, Cliniche Humanitas Gavazzeni, 21 Via Mauro Gavazzeni, Bergamo 24125, Italy
Tel +39 035 420 4663
Fax +39 035 420 4202
Email giovanni_luca.ceresoli@gavazzeni.it

submit your manuscript | www.dovepress.com
Dovepress
http://dx.doi.org/10.2147/LCTT.S102113

reporting. Currently, the recommended classification for clinical use is the TNM staging system established by the International Mesothelioma Interest Group (IMIG) and the International Association for the Study of Lung Cancer (IASLC),[3–6] which is based mainly on surgical and pathological variables, as well as on cross-sectional imaging. Contrast-enhanced computed tomography (CT) is the primary imaging technique for the evaluation of MPM, rind-like extension on pleural surfaces being the most common feature. Magnetic resonance imaging (MRI) is not routinely used in evaluating MPM, but can provide additional staging information in specific scenarios, such as detection of invasion of the chest wall, mediastinum, and diaphragm.[7] Functional imaging with ^{18}F-fluoro-2-deoxy-D-glucose (^{18}F-FDG) positron-emission tomography (PET), integrated with morphological data on CT, has been studied extensively for initial diagnosis and staging of patients with MPM.[8] Moreover, semiquantitative PET parameters have been incorporated into pretreatment prognostic nomograms.[9] Finally, due to the suboptimal accuracy of radiological staging in MPM, some authors have advocated the need for extended surgical staging with mediastinoscopy, contralateral thoracoscopy, and even laparoscopy. The aim of this review is to analyze current literature on clinical staging of patients with MPM, focusing on the most recent achievements, as well as on critical issues.

Prognostic factors

MPM is a heterogeneous disease, often associated with different clinical courses. In the past, a number of prognostic factors have been analyzed, with the aim of improving individual tailoring of treatment strategies. Two major prognostic scoring systems have been published by the European Organization for the Research and Treatment of Cancer (EORTC)[10] and by the Cancer and Leukemia Group B (CALGB).[11] Both models used a training set of treatment-naïve patients enrolled in Phase II trials that were then externally validated.[12–14] The EORTC model identified five variables as independent predictors of poor outcome: male sex, sarcomatoid histology, Eastern Cooperative Oncology Group performance status (PS) >0, white blood cell (WBC) count >8,300/mm^3, and possible/probable diagnosis of MPM (vs definite). Patients were classified into two groups: low risk (0–2 prognostic factors, median survival 10 months) and high risk (3–5 prognostic factors, median survival 5 months).[10] Pleural primary site, LDH >500 U/L, Eastern Cooperative Oncology Group PS >0, platelet count >400,000/mm^3, nonepithelioid histology, and age older than 75 years were independent predictors of poor survival in the CALGB model. Six prognostic subgroups with median survival of 1.4–13.9 months were identified. PS was the most important prognostic split in the regression tree.[11]

Several other prognostic models have been proposed.[9,15–30] Histology (epithelioid vs nonepithelioid) remains the most significant predictor. The negative impact of poor PS, older age, male sex, and laboratory parameters included in the CALGB and EORTC models, such as high platelets and WBC count, have been confirmed as well. Other parameters like neutrophil:lymphocyte ratio,[18,19] albumin,[24] lymphocyte:monocyte ratio, and other inflammatory markers, such as CRP levels[21,28,30] or comorbidities,[25] have been investigated, but none has been included in everyday clinical practice so far. More recently, the expression of B7H1 (PDL1) has been related to nonepithelioid histology and worse overall survival (OS) in several series of MPM;[31–33] however, its potential role as a surrogate marker of response to immunotherapy with immune-checkpoint inhibitors is still debated.

Gordon et al identified a prognostic profile based on the expression of 46 genes.[34] This model was subsequently validated in external MPM cohorts.[35,36] The gene-ratio test, combined with other prognostic factors (histology, lymph-node status) stratified MPM patients undergoing surgery into four distinct groups with OS of 6.9–31.9 months.[36] P16/CDKN2A homozygous deletion, advanced stage, and sarcomatoid histology were independent adverse prognostic factors in another microarray analysis on 80 patients conducted by Lopez-Rios et al.[37]

In recent years, miRNAs have also been identified as potential determinants for diagnosis and prognosis in MPM. Kirschner et al proposed a six-miRNA signature (miR21-5p, miR23a-3p, miR30e-5p, miR221-3p, miR222-3p, miR31-5p) able to predict survival outcomes in surgical patients treated with either extrapleural pneumonectomy or pleurectomy/decortication. The addition of the miRNA signature to a set of selected clinical prognostic criteria increased prognostic accuracy vs a model based on clinical factors only.[38] Other series have reported a correlation between miRNA signature and histologic subtype, or a prognostic association of specific miRNAs (such as miR29c, miR31, miR17-5p and miR30c) within specific histologic subtypes.[39–42]

Molecular reclassifications of MPM subtypes have been proposed, with the aim of overcoming the epithelioid vs nonepithelioid dichotomy and further improving prognostic accuracy. Using a transcriptome microarray analysis, de Reynies et al[43] identified two clusters (C1 and C2). Epithelioid and biphasic subtypes showed heterogeneous distribution, while sarcomatoid samples were found exclusively within the

second cluster, which was related to worse prognosis independently of the histologic subtype. Similarly, Bueno et al[44] defined four molecular categories based on RNA expression: epithelioid (with the longest OS), biphasic epithelioid, biphasic sarcomatoid, and sarcomatoid. Two-thirds of the epithelioid samples were reclassified into other categories. Finally, De Rienzo et al validated a molecular test developed in fresh-frozen tissue using formalin-fixed paraffin-embedded samples from an independent multicenter cohort of surgical patients. Multivariate classification adding pathologic staging information to the gene-expression score resulted in significant stratification of risk groups. Median OS was 52 and 14 months in the low-risk (class 1) and intermediate-risk (class 2) groups, respectively.[45]

TNM classification

Tumor stage remains the most important prognostic factor in many malignancies, and it is often used to stratify patients in clinical trials. In 1995, the IASLC and the IMIG investigators analyzed the available MPM surgical databases and developed a staging system based on TNM.[46] The IMIG–IASLC staging system was accepted by the Union for International Cancer Control and American Joint Committee on Cancer, and since then it has been widely validated and used as an international standard. Nevertheless, this staging system, derived from retrospective surgical series, has shown some limitations when applied to clinically staged patients. In particular, the validity of node descriptors has been questioned. The lymphatic drainage of the pleura is quite complex, and is not fully reflected by the IMIG–IASLC system, in which the N classification mirrors that of lung cancer.

The TNM was updated based on the analysis of an international MPM database. As both clinical and pathological stages were not available for all patients, data were combined to obtain the best TNM. Common clinical variables with validated prognostic impact and TNM parameters were analyzed. Tumor stage, T and N category, histology (epithelioid vs nonepithelioid), sex, age, and type of surgery (curative vs palliative) had a statistically significant impact on OS. Pairwise comparison of stage and T and N categories was statistically significant, with the exception of T1 vs T2, N1 vs N2, and stage I vs stage II. Stage, age, sex, histology, and surgical procedure were defined as core variables.[47] Supplemental prognostic variables were analyzed subsequently.[48] Patients were divided into three groups according to available data: pathological stage available, clinical stage available, and no staging available. Three prognostic models were defined: pathological stage, core variables, adjuvant treatment, platelet and WBC count; clinical stage, core variables, adjuvant treatment, platelet and WBC count, and hemoglobin level; and histology, sex, age, and platelet and WBC count. In the planning of the eighth edition of the American Joint Committee on Cancer and Union for International Cancer Control staging manual, an expansion of the IASLC database was started in 2013.[4] The main changes were related to nodal descriptors.[3,5,6] When N-positive clinically or pathologically staged patients were grouped together, N1 and N2 patients had worse survival compared to N0. No significant differences were seen in patients with single- or multiple-node metastases.[5] Exploratory parameters, such as pleural thickness, presence of N2 skip metastases, number of involved nodes, node ratio and distribution (upper vs lower mediastinal vs nonmediastinal), and site and number of distant metastases were considered as well, but the number of patients included in each group was too small to drive definitive conclusions. Few cM1 cases were included in the database, and their OS was significantly shorter compared to the locally advanced T3–T4 M0 cases.[6] Based on the results of the revision of the database, the main changes proposed in the eighth edition of the TNM classification for MPM were: T1a and T1b grouped in T1; N1 and former N2 grouped in "new" N1, including all homolateral nodes; former N3 nodes classified as N2; and T3 and T4 classified as IIIB, irrespective of N status (Table 1).[4–6]

Radiological imaging

Pleural effusion, pleural thickening, ipsilateral volume loss, local invasion, lymphadenopathy, and metastatic disease are the most common imaging manifestations of MPM. Asbestos-related pleural disease may also be seen. Although individual imaging findings may not be specific, the presence of one or more of these features should raise suspicion for a diagnosis of MPM.

Chest radiography is often the first imaging modality to depict imaging abnormalities of MPM, because of its widespread use and availability. The most common manifestation of MPM is unilateral pleural effusion, reported in up to 80% of patients. Diffuse pleural thickening or pleural masses are observed in 60% and 45%–60% of cases, respectively.[49] Tumors may spread along the interlobar fissures. Encasement of the lung may result in volume loss, which manifests as elevation of the ipsilateral hemidiaphragm, ipsilateral mediastinal shift, and narrowing of the intercostal spaces. Heterologous differentiation is a rare event that occurs particularly in cases of sarcomatoid or biphasic histology. Osseous or chondroid differentiations are the most common ones, and tumors may demonstrate foci of ossification or calcification

Table 1 Eighth edition of the TNM classification for malignant pleural mesothelioma

T1	Tumor involving the ipsilateral parietal or visceral pleura only
T2	Tumor involving ipsilateral pleura (parietal or visceral pleura) with invasion involving at least one of the following: – diaphragmatic muscle – pulmonary parenchyma
T3	Tumor involving ipsilateral pleura (parietal or visceral pleura) with invasion involving at least one of the following: – endothoracic fascia – mediastinal fat – chest wall, with or without associated rib destruction (solitary, resectable) – pericardium (nontransmural invasion)
T4	Tumor involving ipsilateral pleura (parietal or visceral pleura) with invasion involving at least one of the following: – chest wall, with or without associated rib destruction (diffuse or multifocal, unresectable) – peritoneum (via direct transdiaphragmatic extension) – contralateral pleura – mediastinal organs (esophagus, trachea, heart, great vessels) – vertebrae, neuroforamen, spinal cord, or brachial plexus – pericardium (transmural invasion with or without pericardial effusion)
NX	Regional lymph nodes cannot be assessed
N0	No regional lymph-node metastases
N1	Metastases to ipsilateral intrathoracic lymph nodes (including ipsilateral bronchopulmonary, hilar, subcarinal, paratracheal, aortopulmonary, paraesophageal, peridiaphragmatic, pericardial, intercostals, and internal mammary nodes)
N2	Metastases to contralateral intrathoracic lymph nodes, metastases to ipsilateral or contralateral supraclavicular lymph nodes
M0	No distant metastasis
M1	Distant metastases present

Stage	Tumor	Lymph nodes	Metastases
IA	T1	N0	M0
IB	T2, T3	N0	M0
II	T1, T2	N1	M0
IIIA	T3	N1	M0
IIIB	T1–T3	N2	M0
	T4	N0–N2	M0
IV	Any T4	Any N	M1

Note: Data from Pass et al,[3] Nowak et al,[4] Rice et al,[5] and Rusch et al.[6]

that may resemble an osteosarcoma or a chondrosarcoma. Asbestos-related pleural disease may manifest as an indistinct or "shaggy" cardiac silhouette or ill-defined diaphragmatic contours. Intrathoracic lymphadenopathies may manifest on chest radiography as abnormal mediastinal lines and stripes, and normal mediastinal contours may be absent.

Contrast-enhanced chest CT is the imaging modality of choice to evaluate MPM, and demonstrates the extent of primary tumor, local invasion, intrathoracic lymph nodes, and extrathoracic spread. Chest CT alone is often sufficient for disease staging and treatment planning. Unilateral pleural effusion is observed in 74% of cases. Pleural thickening on chest CT can be nodular or lobular, and is seen in up to 92% of patients. Focal or diffuse pleural involvement of more than 1 cm thick is very suggestive of malignant pleural disease, including MPM.[50,51] In cases of MPM with osseous or cartilaginous differentiation, ossification or calcification may be observed in regions of pleural thickening or pleural masses, and the extent of involvement ranges from scattered to diffuse.[52] Calcified pleural plaques representing asbestos-related pleural disease are observed in 20% of patients, and should not be mistaken for osteocartilaginous differentiation. These entities can be differentiated by the shape and location of the mineralization: calcifications associated with pleural plaques are generally linear along the plaque's margins. Osteocartilaginous differentiation usually demonstrates large or punctate foci of mineralization within the tumor. MPM may extend into the mediastinal fat, with loss of fat and tissue planes between mediastinal structures. Encasement bigger than 50% of the circumference of the trachea or esophagus and obliteration of their fat planes are suggestive of mediastinal invasion.[53] Involvement of the pericardium, which may be nontransmural or transmural, may result in pericardial effusion, pericardial thickening, pericardial nodules, and masses. Although differentiating nontransmural from transmural involvement may be difficult, the presence of epicardial fat suggests nontransmural involvement. A tumor that extends to the internal surface of the pericardium or involves the myocardium is consistent with transmural disease. MPM may locally invade the chest wall and manifest as loss of normal

extrapleural fat planes, invasion of intercostal muscles, rib displacement, or osseous destruction (Figure 1). The accuracy of CT for identifying transdiaphragmatic extension remains poor. However, the presence of a distinct fat plane between the inferior surface of the diaphragm and the adjacent abdominal organs is the best indication that MPM is limited to the chest. Tumors with multifocal or diffuse invasion of the chest wall, invasion of the mediastinal structures or spine, transmural invasion of the pericardium, involvement of the contralateral pleura, transdiaphragmatic extension, or metastatic disease are considered unresectable.[53] CT remains one of the primary methods for detecting intrathoracic nodal involvement. Mediastinal lymph nodes, specifically paratracheal, hilar, subcarinal, paraesophageal and para-aortic nodes, that are 10 mm or larger in their short axis are considered abnormal. Internal mammary, retrocrural, and extrapleural lymph nodes have no specific size criteria, and visualization of these nodes is considered pathological. Different patterns of intrathoracic lymphadenopathy can be observed, depending on the location of pleural and diaphragmatic involvement.[54] CT may demonstrate intrathoracic and extrathoracic metastatic disease. Pulmonary metastases may manifest as nodules, masses or lymphangitic carcinomatosis, with thickening and nodularity of the interlobular septa.

Thoracic MRI is not routinely used to evaluate MPM, but may provide more precise staging information in specific scenarios. An advantage of thoracic MRI is its greater sensitivity (in comparison to CT and other imaging modalities) in detecting invasion of the chest wall, mediastinum and diaphragm. MPM may present as a unilateral pleural effusion that is hyperintense on T_2-weighted images. The pleural thickening of MPM is typically isointense to mildly hyperintense compared to muscle on T_1-weighted images and moderately hyperintense compared to muscle on T_2-weighted and proton density-weighted images. Enhancement is typical after administration of intravenous gadolinium-based contrast medium. Thoracic MRI is more accurate than CT for identifying invasion of the chest wall and endothoracic fascia (69% vs 46%) and diaphragmatic invasion (82% vs 55%).[55] In particular, contrast-enhanced T_1-weighted fat-suppressed images were found the most reliable for detecting tumor spread into interlobar fissures and adjacent structures (Figure 2). MRI also offers functional imaging capabilities through diffusion-weighted imaging (DWI), which is an MRI-acquisition protocol that captures water-molecule diffusion within tissues. Since cell membranes restrict water diffusion, a quantity known as the apparent diffusion coefficient (ADC) may be computed from DWI data to represent tissue cellularity, which has been used to differentiate epithelioid and sarcomatoid histologic subtypes in mesothelioma (Figure 3).[56] The ability of ADC to identify the predominant histologic subtype in biphasic MPM tumors is being investigated with prognostic implications; sarcomatoid-dominant biphasic MPM has been shown to have a lower ADC value than epithelioid-dominant biphasic MPM. DWI is further being investigated as a predictive tool in assessing early response to therapy; in fact, ADC has been shown to increase significantly in responders to chemotherapy, radiotherapy, and novel therapeutics as well

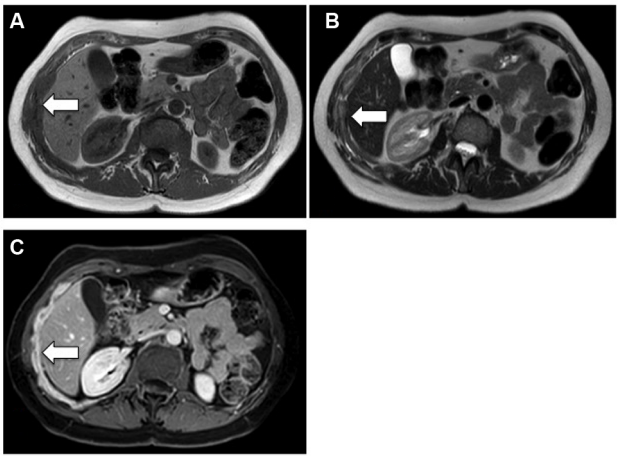

Figure 2 Magnetic resonance imaging (MRI) of a patient with malignant pleural mesothelioma with invasion of the diaphragm (arrows).
Notes: (**A**) Axial T_1-weighted MRI showing pleural thickening that is isointense to muscle in the right hemithorax; (**B**) axial T_2-weighted MRI with hyperintensity of thickened pleura compared to muscle; and (**C**) axial contrast-enhanced T_1-weighted MRI shows diffuse enhancement of the thickened pleura.

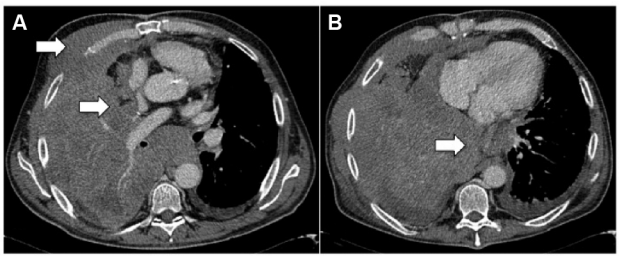

Figure 1 Contrast-enhanced computed tomography showing extensive invasion of the mediastinum, pericardium, and chest wall (arrows).

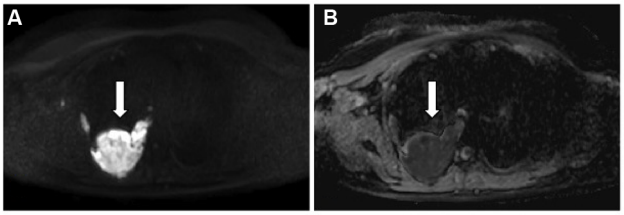

Figure 3 A case of right sarcomatoid malignant pleural mesothelioma (arrows).
Notes: (**A**) Diffusion-weighted image using b=800 s/mm^2 and corresponding (**B**) apparent diffusion-coefficient map demonstrate marked restricted diffusion of the pleural mass.

after embolization across a variety of tumor types.[57] Finally, dynamic contrast-enhanced MRI after the administration of gadolinium can be used to assess perfusion and vascularity of tumors and monitor response to therapy.[58]

Measuring malignant pleural mesothelioma

Currently, the most used measurement system for MPM is the modified Response Evaluation Criteria in Solid Tumors (RECIST) method,[59] which is based on unidimensional measurements of tumor thickness perpendicular to the chest wall or mediastinum measured in two sites at three different levels on CT scan. Transverse cuts used for measurement must be at least 1 cm apart and related to anatomical landmarks in the thorax, preferably above the level of division of the main bronchi. At reassessment, pleural thickness must be measured at the same position and level. Nodal, subcutaneous, and other bidimensionally measurable lesions are measured unidimensionally as per the RECIST criteria.[60] Unidimensional measurements (typically six pleural thickness measurements) are added to produce the total tumor diameter. Lymph nodes are considered a separate organ to measure, and up to two lymph nodes can be measured per patient (Figure 4). The short axis of the lymph node should be considered for measurement at baseline and then at every follow-up scan.

Differential diagnosis

The main differential diagnoses include pleural metastases, pleural dissemination of thymoma, solitary fibrous tumor of the pleura, and epithelioid hemangioendothelioma. Pleural metastases are the most common malignancy of the pleura, and may be indistinguishable from MPM. The most common primary tumors to metastasize to the pleura are lung cancer (40%), breast cancer (20%), lymphoma (10%), and ovarian or gastric cancer (5%). A pseudomesotheliomatous growth pattern can be also observed in lung cancers, especially adenocarcinoma, spreading directly to the pleura. Typical radiological findings of pleural metastases include pleural effusion, pleural thickening, and pleural nodules or masses. Specific immunohistochemistry panels may be helpful in differentiating epithelioid MPM from adenocarcinoma.[61]

Thymoma is the most common primary tumor of the anterior mediastinum. Thymoma with dissemination to the pleura may manifest as pleural thickening and pleural nodules or masses. Invasion of mediastinal fat, cardiovascular structures, pleura, or lung parenchyma may be observed in advanced cases.[62] Solitary fibrous tumors of the pleura are neoplasms that originate from the submesothelial connective tissue and arise from the visceral pleural surface. They are usually benign, but can occasionally have more aggressive behavior. At CT, small lesions are homogeneous, with obtuse margins, but larger lesions can be heterogeneous, with acute margins. These tumors demonstrate heterogeneous signal intensity on both T_1- and T_2-weighted MRI. Because many of these tumors are pedunculated, changes in patient positioning may result in changes in tumor position.[63] Epithelioid hemangioendothelioma is a rare vascular tumor of the lung and liver that may be related to asbestos exposure. These tumors closely mimic MPM and pleural metastases.

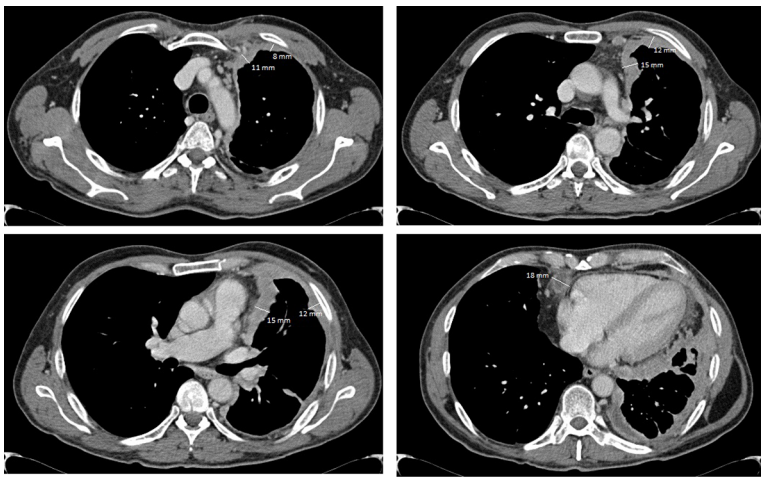

Figure 4 Measurement of MPM according to modified RECIST.
Notes: The total measurement (91 mm) was calculated adding six diameters of pleura tumor thickness (11+8+15+12+15+12 mm) to the short-axis diameter of a lymph node (18 mm).
Abbreviations: MPM, malignant pleural mesothelioma; RECIST, Response Evaluation Criteria in Solid Tumors.

Pleural and pulmonary forms have been described, with poor prognosis associated with the pleural form. Imaging features include loculated pleural effusion, diffuse lobular pleural thickening, and pleural masses.[64]

Metabolic imaging

Diagnosis and staging

Functional imaging with ^{18}F-FDG PET integrated with morphological data on CT is regarded as very useful for initial diagnosis and preoperative staging of patients with MPM. In vitro studies have shown significantly increased FDG uptake in most tumor cell lines, and positive correlations among proliferative index, tumor aggression, and FDG uptake have been observed in several malignancies, including MPM.[65–67] Several clinical investigations have analyzed the diagnostic accuracy of ^{18}F-FDG PET and PET/CT in differentiating malignant lesions from benign pleural diseases (Table 2).[68–76] Overall, either by pure visual analysis or by applying semiquantitative parameters on PET (ie, maximum standardized uptake value [SUV_{max}]), the accuracy of the method varies from 91% to 98%.[72,74,76] Optimal cutoff values for FDG uptake have been defined, ranging from 2[69] to 3.5.[77] In an early study, Benard et al[69] examined 28 consecutive patients with suspected malignant mesothelioma. Of these, 24 were confirmed as malignant, showing a highly significant increase in FDG uptake compared to benign lesions. By using an SUV_{max} cutoff of 2, the authors reported sensitivity of 91% and specificity of 100%. In larger series investigating pleural diseases,[74] SUV_{max} ≥3 discriminated malignancies from benign pleural lesions with 100% sensitivity, 94.8% specificity, and 97.5% accuracy. In other cases,[68,75] pure visual assessment reached sensitivity of 95%–97% and accuracy of 94%. This latter modality, as confirmed in a recent meta-analysis by Porcel et al,[78] who pooled data derived from 639 patients, is expected to perform even better in terms of sensitivity (91% vs 82%, P=0.026) compared to semiquantitative analyses. Whatever the modality used, if we simply compare these findings with typical CT features used to differentiate malignant from benign pleural disease, ie, pleural thickening encasing the lung (sensitivity 100%, specificity 41%), pleural thickening >1 cm (sensitivity 94%, specificity 36%), and nodular pleural thickening (sensitivity 94%, specificity 51%), the superiority of functional imaging is clearly seen.[79,80] However, a diagnosis of MPM must still rely on histopathological confirmation by video-assisted thoracoscopy, or by CT-guided biopsy, when thoracoscopy is not feasible.[81] Video-assisted thoracoscopy has a diagnostic performance of up to 98%, and is regarded better to estimate the pleural extent of MPM lesions compared to ^{18}F-FDG PET/CT alone, especially for very limited disease and epithelioid histology, commonly presenting with lower FDG uptake.[66,80,82] On the contrary, for extrathoracic metastases, the incidence of which is reported in about 50%–80% of cases in autoptic series,[83] whole-body imaging with ^{18}F-FDG PET/CT is to be considered the optimal modality for MPM staging (Figures 5 and 6).

Numerous studies have been published on pretreatment MPM assessment with PET, either alone or in comparison with other imaging modalities. Findings have not been univocal, since diagnostic performance has shown a large range between different authors. Gerbaudo et al[84] reported an overall accuracy of 94% (sensitivity 97%, specificity 80%). Agreement with tumor biopsy was very high (94%, κ=0.77), better than with CT (82%, κ=0.47; P<0.0001). In addition, the sensitivity for diffuse chest disease, mediastinal lymph nodes, and extrathoracic metastases was 100%, 88%, and 100%, respectively. Plathow et al[85] compared PET alone and PET/CT, revealing higher diagnostic performance of the latter modality in all MPM stages (accuracy 83%–100% for PET and 100% for PET/CT). On the contrary, other studies[86,87] have reported disappointing results for nodal staging in MPM patients (sensitivity 11% and 38%, respectively). Sørensen et al[88]compared CT, PET/CT, and mediastinoscopy in 42 patients undergoing preoperative staging after three to six courses of induction chemotherapy. For N2/N3 nodal stations, FDG PET/CT showed sensitivity, specificity, positive predictive value, and negative predictive value of 78%, 50%, 100%, and 75%, respectively. In the same cohort, mediastinoscopy showed rates of 100%, 50%, 94%, and 75%. As a result, inadequate surgery was avoided in 29% of MPM patients by PET/CT and in a further 14% of cases by mediastinoscopy.[88] Overall, the use of ^{18}F-FDG PET/CT vs CT imaging led to a change in patient management in nearly 20%–40% of MPM patients.[88–91]

PET and MPM prognosis

Tumor avidity for FDG has been investigated as a surrogate marker of MPM biology. Nowak et al[9] incorporated semiquantitative PET parameters and pleurodesis into pretreatment predictors, proposing a prognostic nomogram for MPM. Other authors have confirmed that pretreatment PET parameters are robust predictors of survival in MPM patients, with SUV_{max} or volume-based analyses (ie, metabolic tumor volume, total glycolytic volume, and total lesion glycolysis [TLG]) and histology being the main independent prognostic factors.[92–98] Flores et al incorporated SUV_{max} into a prognostic

Table 2 FDG PET and PET/CT in MPM

Study	Type	Population	Setting	Modality	Results
Benard et al[69]	Retrospective	28 (24 MPM, four benign pleural lesions)	Diagnosis	PET	SENS 92%, SPEC 75%, ACC 89%; FDG uptake malignant vs benign lesions 4.9±2.9 vs 1.4±0.6 (P<0.0001); SENS 91% and SPEC 100%, with an SUV cutoff of 2 to differentiate between malignant and benign disease
Yamamoto et al[70]	Retrospective	33 (17 MPM, 16 benign pleural lesions)	Diagnosis	PET	SENS, SPEC, ACC 88%; mean SUV values significantly higher in MPM than benign pleural disease (P<0.01)
Flores[86]	Retrospective	68 (all MPM)	Diagnosis/staging	PET	ACC 98.3%; AUC for N2 detection 78%±10%; detection of T4 SENS 19%, SPEC 91%; detection of extrathoracic disease ACC 66.7%
Yildrim et al[72]	Retrospective	31 (17 MPM, nine benign asbestos pleurisies, five pleural fibrosis)	Diagnosis	PET/CT	SENS 88.2%, SPEC 92.9%, ACC 90.3%; mean SUV, MPM 6.5±3.4 vs benign pleural diseases 0.8±0.6 (P<0.001); cutoff value of 2.2 for SUV gave the best accuracy
Tan et al[73]	Retrospective	25 (all MPM after EPP or P/D)	Follow-up	PET/CT	Detection of recurrences: SENS 94%, SPEC 100%
Erasmus et al[87]	Retrospective	29 (all MPM candidates for EPP after radiological evaluation)	Staging	PET/CT	Overall T, ACC 63%; T4 detection, SENS 67%, SPEC 93%, ACC 83%; overall N accuracy 32%; N2 detection, SENS 38%, SPEC 78%, ACC 59%; in eleven patients, PET/CT provided additional information that precluded EPP
Gerbaudo et al[84]	Retrospective	15 (eleven MPM, four benign disease)	Diagnosis	FDG-CI	Overall ACC 94%, SENS 97%, SPEC 80% (vs CT 82%, 83%, 80%, respectively); agreement with biopsy 94% vs CT 82% (P<0.0001); detection of diffuse chest disease 100%, mediastinal LNs 88%, extrathoracic metastases 100% (vs CT 33%, 75%, 100%, respectively)
Nanni et al[91]	Retrospective	15 (all MPM, five staging, ten follow-up)	Staging/follow-up	PET	Concordance PET and CT, overall 60% (exact TNM match 27%); PET upstaged two patients (13%) and downstaged four (27%)
Plathow et al[85]	Retrospective	54 (all MPM candidates for surgery)	Staging	PET and PET/CT	Overall ACC, PET 83%–100%, PET/CT 100%; stage-specific ACC, stage II, PET 86%, PET/CT 100% (P<0.05, P<0.01 vs CT, P<0.05 vs MRI); stage III, PET 83%, PET/CT 100% (P<0.05, P<0.01 vs CT, P<0.05 vs MRI); stage IV, PET 100%, PET/CT 100%; stage II, SENS and SPEC PET 100% and 84.6%, PET/CT 100% and 100%; stage III, SENS and SPEC, PET 83% and 100%, PET/CT 100% and 100%
Ambrosini et al[89]	Retrospective	15 (all MPM)	Staging	PET/CT	PET/CT did not provide additional information about the primary tumor vs CT scan, but identified a higher number of metastatic mediastinal LNs in six patients (40%) and unknown metastatic disease in three patients (20%)
Orki et al[74]	Prospective	83 (44 malignant disease of which 25 MPM, 39 benign)	Diagnosis	PET/CT	SENS 100%, SPEC 94.8%, ACC 97.5%
Sørensen et al[88]	Prospective	42 (all MPM candidates for surgery)	Staging	PET/CT	T4 and N2/N3, SENS 78%, spec 50%; noncurative surgery avoided in 29 of 42 MPM by preoperative PET/CT (further 14% by mediastinoscopy)

Abbreviations: MPM, malignant pleural mesothelioma; CT, computed tomography; PET, positron-emission tomography; FDG, fluorodeoxyglucose; SUV, standardized uptake value; CI, coincidence imaging; EPP, extrapleural pneumonectomy; P/D pleurectomy/decortication; LNs, lymph nodes; ADC, adenocarcinoma; SENS, sensibility; SPEC, specificity; ACC accuracy; AUC, area under the curve.

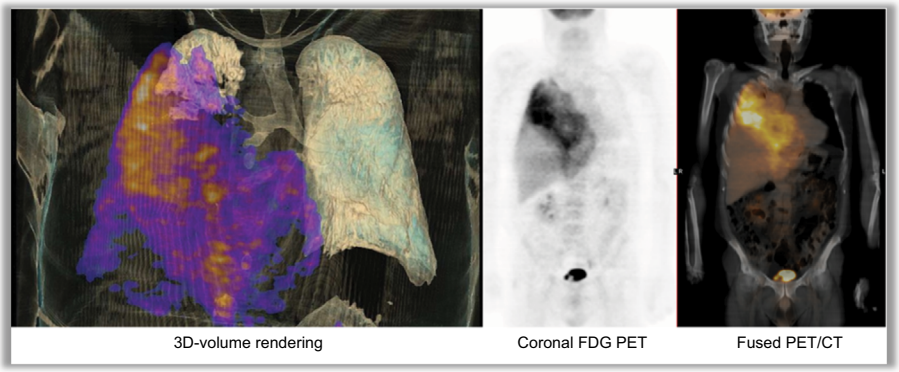

Figure 5 FDG-PET images of a patient affected by MPM, including three-dimensional rendering.
Abbreviations: FDG, fluorodeoxyglucose; PET, positron-emission tomography; MPM, malignant pleural mesothelioma.

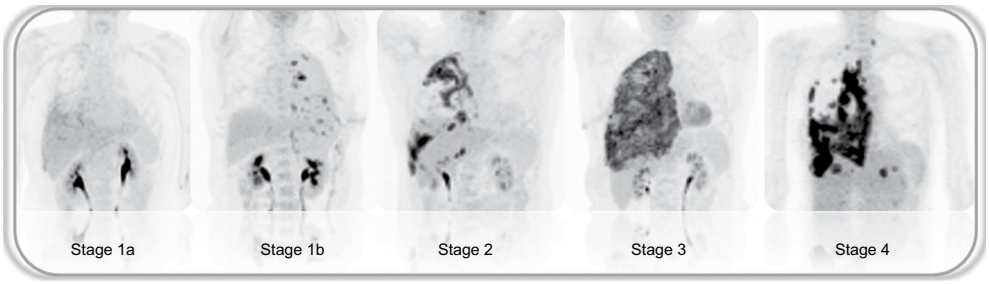

Figure 6 Maximal-intensity projection of FDG-PET in five different MPM patient presenting with various stages of disease extension.
Abbreviations: FDG, fluorodeoxyglucose; PET, positron-emission tomography; MPM, malignant pleural mesothelioma.

model with stage and histology, observing that SUV >10 MPM were associated with poor prognosis.[94] According to Terada et al,[77] SUV_{max} >3.5 might identify patients with poor prognosis. Similarly, SUV_{max} was an independent predictor of survival in two other patient series, with cutoff values of 10.7 and 5, respectively.[92,95] Recently, TLG and histology were confirmed as independent prognostic factors in MPM patients by Klabatsa et al.[93] Finally, Lee et al[96] reported lower SUV_{max} of primary pleural lesions in patients with locoregional disease only compared to patients with metastatic disease. The same authors[97] reported metabolic tumor volume (HR 1.003, P=0.025) and TLG (HR 1.001, P=0.031) as independent factors associated with MPM progression.[98]

Impact of pleurodesis and inflammation

Talc pleurodesis is a common procedure in MPM patients presenting with pleural effusion. The aim of this treatment relies on the chemical irritation and pleural fibrosis following talc instillation, which leads to the adherence of pleural layers.[99] Pleurodesis causes intensive inflammation and massive recruitment of immune cells. Markedly increased FDG uptake characterizes the process, which can persist for an unpredictable period (Figure 7).[100–102] Several authors[103–106] have reported the presence of focal and/or diffused tracer accumulation visible on partially calcified pleural thickening years (up to decades) following pleurodesis. Since only 10% of pleural malignancies present with calcifications, major help in the identification of these cases is given by proper anamnesis and by the identification on CT images of concordance/overlap between FDG-avid lesions and highly CT-attenuated areas.[99,104–106] The negative impact of FDG uptake induced by pleurodesis is seen at initial staging, as well as at response assessment, since the effective extent of MPM can be overestimated by the contemporary presence of pleural granulomatous reaction to talc.

FDG is not cancer-specific, and can be actively accumulated in several inflammatory processes, such as primary tuberculous pleurisy.[107] Use of semiquantitative parameters can help in partially overcoming the issue of false-positive uptake, since in the majority of cases mean SUV in malignant lesions is significantly higher than in benign processes,[72] although some overlap in the UV, particularly in cases of limited MPM lesions and epithelioid histology, is possible.[66,67,82] Use of delayed imaging, ie, 90–120 minutes after tracer injection,[71,76,108] increases the diagnostic accuracy of PET/CT. Usually, FDG accumulation in inflammation decreases

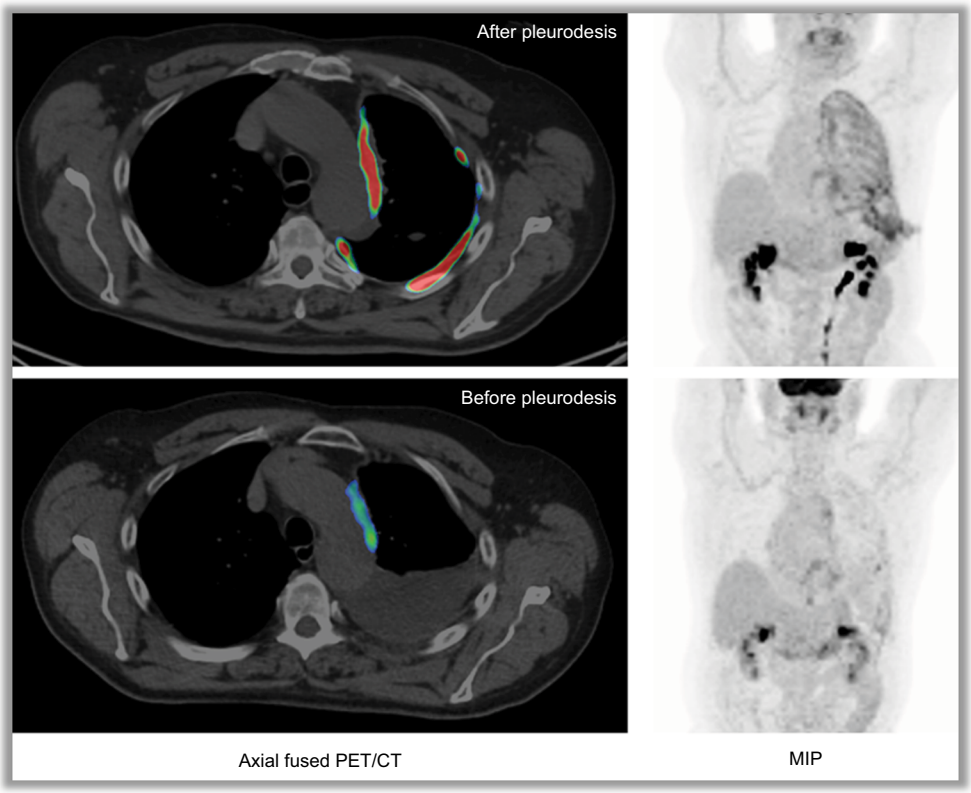

Figure 7 Impact of talc pleurodesis on FDG uptake.
Note: Images represent the same MPM patient investigated before (lower panel) and after talc pleurodesis (upper panel).
Abbreviations: FDG, fluorodeoxyglucose; MPM, malignant pleural mesothelioma; PET, positron-emission tomography; CT, computed tomography; MIP, maximal-intensity projection.

over time, while malignant lesions present increased uptake on delayed images compared to standard acquisition at 60 minutes. The rationale for these findings is based on the fact that tumor cells have higher levels of hexokinase, responsible for intracellular entrapment of FDG, and lower levels of glucose-6-phosphatase, which is supposed to revert the process of phosphorylation and permit the backflow of the tracer outside the tumor cell.[80]

Conclusion

Clinical staging and prognostication of MPM remain challenging. The TNM staging system has been recently updated to overcome the main limitations of previous editions, such as the evaluation of N descriptors and site and number of distant metastases. Beyond TNM, histology remains the most important determinant for prognosis. Overall, novel tools are much needed to improve patient selection for more personalized and effective treatments. New imaging techniques, such as volumetric tumor measurement with CT scan, MRI-specific imaging-acquisition protocols, and semiquantitative PET parameters, are being implemented in the research setting, and hopefully will soon be integrated into clinical practice. Molecular reclassification of MPM and gene-expression or miRNA prognostic models seem promising, but results still need to be validated in large prospective series.

Acknowledgment

LG is supported by Fondazione Buzzi Unicem Onlus.

Disclosure

The authors report no conflicts of interest in this work.

References

1. Baas P, Fennell D, Kerr KM, Van Schil PE, Haas RL, Peters S. Malignant pleural mesothelioma: ESMO clinical practice guidelines for diagnosis, treatment and follow-up. *Ann Oncol*. 2015;26 Suppl 5:v31–v39.
2. Galateau-Salle F, Churg A, Roggli V, Travis WD. The 2015 World Health Organization classification of tumors of the pleura: advances since the 2004 classification. *J Thorac Oncol*. 2016;11:142–154.
3. Pass H, Giroux D, Kennedy C, et al. The IASLC Mesothelioma Staging Project: improving staging of a rare disease through international participation. *J Thorac Oncol*. 2016;11:2082–2088.
4. Nowak AK, Chansky K, Rice DC, et al. The IASLC Mesothelioma Staging Project: proposals for revisions of the T descriptors in the forthcoming eighth edition of the TNM classification for pleural mesothelioma. *J Thorac Oncol*. 2016;11:2089–2099.

5. Rice D, Chansky K, Nowak A, et al. The IASLC Mesothelioma Staging Project: proposals for revisions of the N descriptors in the forthcoming eighth edition of the TNM classification for pleural mesothelioma. *J Thorac Oncol*. 2016;11:2100–2111.
6. Rusch VW, Chansky K, Kindler HL, et al. The IASLC Mesothelioma Staging Project: proposals for the M descriptors and for revision of the TNM stage groupings in the forthcoming (eighth) edition of the TNM classification for mesothelioma. *J Thorac Oncol*. 2016;11:2112–2119.
7. Truong MT, Viswanathan C, Godoy MB, Carter BW, Marom EM. Malignant pleural mesothelioma: role of CT, MRI, and PET/CT in staging evaluation and treatment considerations. *Semin Roentgenol*. 2013;48:323–334.
8. Kitajima K, Doi H, Kuribayashi K. Present and future roles of FDG-PET/CT imaging in the management of malignant pleural mesothelioma. *Jpn J Radiol*. 2016;34:537–547.
9. Nowak AK, Francis RJ, Phillips MJ, et al. A novel prognostic model for malignant mesothelioma incorporating quantitative FDG-PET imaging with clinical parameters. *Clin Cancer Res*. 2010;16:2409–2417.
10. Curran D, Sahmoud T, Therasse P, van Meerbeeck J, Postmus PE, Giaccone G. Prognostic factors in patients with pleural mesothelioma: the European Organization for Research and Treatment of Cancer experience. *J Clin Oncol*. 1998;16:145–152.
11. Herndon JE, Green MR, Chahinian AP, Corson JM, Suzuki Y, Vogelzang NJ. Factors predictive of survival among 337 patients with mesothelioma treated between 1984 and 1994 by the Cancer and Leukemia Group B. *Chest*. 1998;113:723–731.
12. Edwards JG, Abrams KR, Leverment JN, Spyt TJ, Waller DA, O'Byrne KJ. Prognostic factors for malignant mesothelioma in 142 patients: validation of CALGB and EORTC prognostic scoring systems. *Thorax*. 2000;55:731–735.
13. Fennell DA, Parmar A, Shamash J, et al. Statistical validation of the EORTC prognostic model for malignant pleural mesothelioma based on three consecutive phase II trials. *J Clin Oncol*. 2005;23:184–189.
14. Sandri A, Guerrera F, Roffinella M, et al. Validation of EORTC and CALGB prognostic models in surgical patients submitted to diagnostic, palliative or curative surgery for malignant pleural mesothelioma. *J Thorac Dis*. 2016;8:2121–2127.
15. Neumann V, Rütten A, Scharmach M, Müller KM, Fischer M. Factors influencing long-term survival in mesothelioma patients: results of the German mesothelioma register. *Int Arch Occup Environ Health*. 2004;77:191–199.
16. Francart J, Vaes E, Henrard S, et al. A prognostic index for progression-free survival in malignant mesothelioma with application to the design of phase II trials: a combined analysis of 10 EORTC trials. *Eur J Cancer*. 2009;45:2304–2311.
17. Yan TD, Boyer M, Tin MM, et al. Prognostic features of long-term survivors after surgical management of malignant pleural mesothelioma. *Ann Thorac Surg*. 2009;87:1552–1556.
18. Kao SC, Pavlakis N, Harvie R, et al. High blood neutrophil-to-lymphocyte ratio is an indicator of poor prognosis in malignant mesothelioma patients undergoing systemic therapy. *Clin Cancer Res*. 2010;16:5805–5813.
19. Kao SC, Klebe S, Henderson DW, et al. Low calretinin expression and high neutrophil-to-lymphocyte ratio are poor prognostic factors in patients with malignant mesothelioma undergoing extrapleural pneumonectomy. *J Thorac Oncol*. 2011;6:1923–1929.
20. Nojiri S, Gemba K, Aoe K, et al. Survival and prognostic factors in malignant pleural mesothelioma: a retrospective study of 314 patients in the west part of Japan. *Jpn J Clin Oncol*. 2011;41:32–39.
21. Pinato DJ, Mauri FA, Ramakrishnan R, Wahab L, Lloyd T, Sharma R. Inflammation-based prognostic indices in malignant pleural mesothelioma. *J Thorac Oncol*. 2012;7:587–594.
22. Baud M, Strano S, Dechartres A, et al. Outcome and prognostic factors of pleural mesothelioma after surgical diagnosis and/or pleurodesis. *J Thorac Cardiovasc Surg*. 2013;145:1305–1311.
23. Kao SC, Vardy J, Chatfield M, et al. Validation of prognostic factors in malignant pleural mesothelioma: a retrospective analysis of data from patients seeking compensation from the New South Wales Dust Diseases Board. *Clin Lung Cancer*. 2013;14:70–77.
24. Murphy S, Probert G, Anderson J, et al. Malignant mesothelioma, hypoalbuminaemia and the effect of carboplatin/pemetrexed on survival. *Clin Oncol (R Coll Radiol)*. 2013;25:713–718.
25. Ceresoli GL, Grosso F, Zucali PA, et al. Prognostic factors in elderly patients with malignant pleural mesothelioma: results of a multicenter survey. *Br J Cancer*. 2014;111:220–226.
26. Linton A, Pavlakis N, O'Connell R, et al. Factors associated with survival in a large series of patients with malignant pleural mesothelioma in New South Wales. *Br J Cancer*. 2014;111:1860–1869.
27. Kataoka Y, Yamamoto Y, Otsuki T, et al. A new prognostic index for overall survival in malignant pleural mesothelioma: the rPHS (regimen, PS, histology or stage) index. *Jpn J Clin Oncol*. 2015;45:562–568.
28. Yamagishi T, Fujimoto N, Nishi H, et al. Prognostic significance of the lymphocyte-to-monocyte ratio in patients with malignant pleural mesothelioma. *Lung Cancer*. 2015;90:111–117.
29. Bille A, Krug LM, Woo KM, Rusch VW, Zauderer MG. Contemporary analysis of prognostic factors in patients with unresectable malignant pleural mesothelioma. *J Thorac Oncol*. 2016;11:249–255.
30. Tanrikulu AC, Abakay A, Komek H, Abakay O. Prognostic value of the lymphocyte-to-monocyte ratio and other inflammatory markers in malignant pleural mesothelioma. *Environ Health Prev Med*. 2016;21:304–311.
31. Mansfield AS, Roden AC, Peikert T, et al. B7-H1 expression in malignant pleural mesothelioma is associated with sarcomatoid histology and poor prognosis. *J Thorac Oncol*. 2014;9:1036–1040.
32. Cedrés S, Ponce-Aix S, Zugazagoitia J, et al. Analysis of expression of programmed cell death 1 ligand 1 (PD-L1) in malignant pleural mesothelioma (MPM). *PLoS One*. 2015;10:e0121071.
33. Thapa B, Salcedo A, Lin X, et al. The immune microenvironment, genome-wide copy number aberrations, and survival in mesothelioma. *J Thorac Oncol*. 2017;12:850–859.
34. Gordon GJ, Jensen RV, Hsiao LL, et al. Using gene expression ratios to predict outcome among patients with mesothelioma. *J Natl Cancer Inst*. 2003;95:598–605.
35. Gordon GJ, Rockwell GN, Godfrey PA, et al. Validation of genomics-based prognostic tests in malignant pleural mesothelioma. *Clin Cancer Res*. 2005;11:4406–4414.
36. Gordon GJ, Dong L, Yeap BY, et al. Four-gene expression ratio test for survival in patients undergoing surgery for mesothelioma. *J Natl Cancer Inst*. 2009;101:678–686.
37. Lopez-Rios F, Chuai S, Flores R, et al. Global gene expression profiling of pleural mesotheliomas: overexpression of aurora kinases and P16/CDKN2A deletion as prognostic factors and critical evaluation of microarray-based prognostic prediction. *Cancer Res*. 2006;66:2970–2979.
38. Kirschner MB, Cheng YY, Armstrong NJ, et al. MiR-score: a novel 6-microRNA signature that predicts survival outcomes in patients with malignant pleural mesothelioma. *Mol Oncol*. 2015;9:715–726.
39. Lamberti M, Capasso R, Lombardi A, et al. Two different serum MiRNA signatures correlate with the clinical outcome and histological subtype in pleural malignant mesothelioma patients. *PLoS One*. 2015;10:e0135331.
40. Pass HI, Goparaju C, Ivanov S, et al. Hsa-miR-29c* is linked to the prognosis of malignant pleural mesothelioma. *Cancer Res*. 2010;70:1916–1924.
41. Matsumoto S, Nabeshima K, Hamasaki M, Shibuta T, Umemura T. Upregulation of microRNA-31 associates with a poor prognosis of malignant pleural mesothelioma with sarcomatoid component. *Med Oncol*. 2014;31:303.
42. Busacca S, Germano S, De Cecco L, et al. MicroRNA signature of malignant mesothelioma with potential diagnostic and prognostic implications. *Am J Respir Cell Mol Biol*. 2010;42:312–319.

43. de Reynies A, Jaurand MC, Renier A, et al. Molecular classification of malignant pleural mesothelioma: identification of a poor prognosis subgroup linked to the epithelial-to-mesenchymal transition. *Clin Cancer Res*. 2014;20:1323–1334.
44. Bueno R, Stawiski EW, Goldstein LD, et al. Comprehensive genomic analysis of malignant pleural mesothelioma identifies recurrent mutations, gene fusions and splicing alterations. *Nat Genet*. 2016;48:407–416.
45. De Rienzo A, Cook RW, Gustafson CE, et al. Validation of a gene expression test for mesothelioma prognosis in formalin-fixed paraffin-embedded tissues. *J Mol Diagn*. 2017;19:65–71.
46. Rusch VW. A proposed new international TNM staging system for malignant pleural mesothelioma. *Chest*. 1995;108:1122–1128.
47. Rusch VW, Giroux D, Kennedy C, et al. Initial analysis of the International Association for the Study of Lung Cancer mesothelioma database. *J Thorac Oncol*. 2012;7:1631–1639.
48. Pass HI, Giroux D, Kennedy C, et al. Supplementary prognostic variables for pleural mesothelioma: a report from the IASLC staging committee. *J Thorac Oncol*. 2014;9:856–864.
49. Wechsler RJ, Rao VM, Steiner RM. The radiology of thoracic malignant mesothelioma. *Crit Rev Diagn Imaging*. 1984;20:283–310.
50. Kawashima A, Libshitz HI. Malignant pleural mesothelioma: CT manifestations in 50 cases. *AJR Am J Roentgenol*. 1990;155:965–969.
51. Leung AN, Müller NL, Miller RR. CT in differential diagnosis of diffuse pleural disease. *AJR Am J Roentgenol*. 1990;154:487–492.
52. Shiba N, Kusumoto M, Tsuta K, et al. A case of malignant pleural mesothelioma with osseous and cartilaginous differentiation. *J Thorac Imaging*. 2011;26:30–32.
53. Patz EF Jr, Shaffer K, Piwnica-Worms DR, et al. Malignant pleural mesothelioma: value of CT and MR imaging in predicting resectability. *AJR Am J Roentgenol*. 1992;159:961–966.
54. Sharma A, Fidias P, Hayman LA, Loomis SL, Taber KH, Aquino SL. Patterns of lymphadenopathy in thoracic malignancies. *Radiographics*. 2004;24:419–434.
55. Heelan RT, Rusch VW, Begg CB, Panicek DM, Caravelli JF, Eisen C. Staging of malignant pleural mesothelioma: comparison of CT and MR imaging. *AJR Am J Roentgenol*. 1999;172:1039–1047.
56. Gill RR, Umeoka S, Mamata H, et al. Diffusion-weighted MRI of malignant pleural mesothelioma: preliminary assessment of apparent diffusion coefficient in histologic subtypes. *AJR Am J Roentgenol*. 2010;195:W125–W130.
57. Armato SG 3rd, Coolen J, Nowak AK, et al. Imaging in pleural mesothelioma: a review of the 12th International Conference of the International Mesothelioma Interest Group. *Lung Cancer*. 2015;90:148–54.
58. Giesel FL, Bischoff H, von Tengg-Kobligk H, et al. Dynamic contrast-enhanced MRI of malignant pleural mesothelioma: a feasibility study of noninvasive assessment, therapeutic follow-up, and possible predictor of improved outcome. *Chest*. 2006;129:1570–1576.
59. Byrne MJ, Nowak AK. Modified RECIST criteria for assessment of response in malignant pleural mesothelioma. *Ann Oncol*. 2004;15:257–260.
60. Eisenhauer EA, Therasse P, Bogaerts J, et al. New response evaluation criteria in solid tumours: revised RECIST guideline (version 1.1). *Eur J Cancer*. 2009;45:228–247.
61. Chirieac LR, Corson JM. Pathologic evaluation of malignant pleural mesothelioma. *Semin Thorac Cardiovasc Surg*. 2009;21:121–124.
62. Benveniste MF, Rosado-de-Christenson ML, Sabloff BS, Moran CA, Swisher SG, Marom EM. Role of imaging in the diagnosis, staging, and treatment of thymoma. *Radiographics*. 2011;31:1847–1861.
63. Keraliya AR, Tirumani SH, Shinagare AB, Zaheer A, Ramaiya NH. Solitary fibrous tumors: 2016 imaging update. *Radiol Clin North Am*. 2016;54:565–579.
64. Kim EY, Kim TS, Han J, Choi JY, Kwon OJ, Kim J. Thoracic epithelioid hemangioendothelioma: imaging and pathologic features. *Acta Radiol*. 2011;52:161–166.
65. Haberkorn U. Positron emission tomography in the diagnosis of mesothelioma. *Lung Cancer*. 2004;45S:S73–S76.
66. Kadota K, Kachala SS, Nitadori J, et al. High SUV_{max} on FDG-PET indicates pleomorphic subtype in epithelioid malignant pleural mesothelioma: supportive evidence to reclassify pleomorphic as nonepithelioid histology. *J Thorac Oncol*. 2012;7:1192–1197.
67. Krüger S, Pauls S, Mottaghy FM, et al. Integrated FDG PET-CT imaging improves staging in malignant pleural mesothelioma. *Nuklearmedizin*. 2007;46:239–243.
68. Duysinx B, Nguyen D, Louis R, et al. Evaluation of pleural disease with 18-fluorodeoxyglucose positron emission tomography imaging. *Chest*. 2004;125:489–493.
69. Benard F, Sterman D, Smith RJ, Kaiser LR, Albeda SM, Alavi A. Metabolic imaging of malignant pleural mesothelioma with fluorodeoxyglucose positron emission tomography. Chest. 1998;9:713–722.
70. Yamamoto Y, Kameyama R, Togami T, et al. Dual time point FDG PET for evaluation of malignant pleural mesothelioma. *Nucl Med Commun*. 2009;1:25–29.
71. Mavi A, Basu S, Cermik TF, et al. Potential of dual time point FDG-PET imaging in differentiating malignant from benign pleural disease. *Mol Imaging Biol*. 2009;5:369–378.
72. Yildrim H, Metintas M, Entok E, et al. Clinical value of fluorodeoxyglucose-positron emission tomography computed tomography in differentiation of malignant mesothelioma from asbestos-related benign pleural disease. *J Thorac Oncol*. 2009;12:1480–1484.
73. Tan C, Barrington S, Rankin S, et al. Role of integrated 18-fluorodeoxyglucose positron emission tomography-computed tomography in patients [sic] surveillance after multimodality therapy of malignant pleural mesothelioma. *J Thorac Oncol*. 2010;3:385–388.
74. Orki A, Akin O, Tasci AE, et al. The role of positron emission tomography/computed tomography in the diagnosis of pleural diseases. *Thorac Cardiovasc Surg*. 2009;57:217–221.
75. Kramer H, Pieterman RM, Slebos DJ, et al. PET for the evaluation of pleural thickening observed on CT. *J Nucl Med*. 2004;45:995–998.
76. Abe Y, Tamura K, Sakata I, et al. Clinical implications of ^{18}F-fluorodeoxyglucose positron emission tomography/computed tomography at delayed phase for diagnosis and prognosis of malignant pleural mesothelioma. *Oncol Rep*. 2012;27:333–338.
77. Terada T, Tabata C, Tabata R, et al. Clinical utility of 18-fluorodeoxyglucose positron emission tomography/computed tomography in malignant pleural mesothelioma. *Exp Ther Med*. 2012;4:197–200.
78. Porcel JM, Hernández P, Martínez-Alonso M, Bielsa S, Salud A. Accuracy of fluorodeoxyglucose-PET imaging for differentiating benign from malignant pleural effusions: a meta-analysis. *Chest*. 2015;147:502–512.
79. Leung AN, Müller NL, Miller RR. CT in differential diagnosis of diffuse pleural disease. *AJR Am J Roentgenol*. 1990;154:487–492.
80. Truong MT, Viswanathan C, Godoy MBC, Carter BW, Marom EM. malignant pleural mesothelioma: role of CT, MRI, and PET/CT in staging evaluation and treatment considerations. *Semin Roentgenol*. 2013;48:323–334.
81. Metintas M, Ozdemir N, Isiksoy S, et al. CT-guided pleural needle biopsy in the diagnosis of malignant mesothelioma. *J Comput Assist Tomogr*. 1995;19:370–374.
82. Roca E, Laroumagne S, Vandemoortele T, et al. ^{18}F-fluoro-2-deoxy-d-glucose positron emission tomography/computed tomography fused imaging in malignant mesothelioma patients: looking from outside is not enough. *Lung Cancer*. 2013;79:187–90.
83. Pass HI, Kranda K, Temeck BK, et al. Surgically debulked malignant pleural mesothelioma: results and prognostic factors. *Ann Surg Oncol*. 1997;4:215–222.
84. Gerbaudo VH, Sugarbaker DJ, Britz-Cunningham S, Di Carli MF, Mauceri C, Treves ST. Assessment of malignant pleural mesothelioma with ^{18}F-FDG dual-head gamma-camera coincidence imaging: comparison with histopathology. *J Nucl Med*. 2002;9:1144–1149.
85. Plathow C, Staab A, Schmaehl A, et al. Computed tomography, positron emission tomography-computed tomography and magnetic resonance imaging for staging of limited pleural mesothelioma. *Invest Radiol*. 2008;10:737–744.

86. Flores R. The role of PET in the surgical management of malignant pleural mesothelioma. *Lung Cancer*. 2005;7:S27–S32.
87. Erasmus JJ, Truong MT, Smythe WR, et al. Integrated computed-tomography in patients with potentially resectable malignant pleural mesothelioma: staging implications. *J Thorac Cardiovasc Surg*. 2005;6:1364–1370.
88. Sørensen JB, Ravn J, Loft A, Brenøe J, Berthelsen AK. Preoperative staging of mesothelioma by ^{18}F-fluoro-2-deoxy-D-glucose positron emission tomography/computed tomography fused imaging and mediastinoscopy compared to pathological findings after extrapleural pneumonectomy. *Eur J Cardiothorac Surg*. 2008;34:1090–1096.
89. Ambrosini V, Rubello D, Nanni C, et al. Additional value of hybrid PET/CT fusion imaging vs conventional CT scan alone in the staging and management of patients with malignant pleural mesothelioma. *Nucl Med Rev*. 2005;8:111–115.
90. Wilcox BE, Subramaniam RM, Peller PJ, et al. Utility of integrated computed tomography-positron emission tomography for selection of operable malignant pleural mesothelioma. *Clin Lung Cancer*. 2009;10:244–248.
91. Nanni C, Castellucci P, Farsad M, et al. Role of ^{18}F-FDG PET for evaluating malignant pleural mesothelioma. *Cancer Biother Radiopharm*. 2004;4:149–154.
92. Abakay A, Komek H, Abakay O, et al. Relationship between 18 FDG PET-CT findings and survival of 177 patients with malignant pleural mesothelioma. *Eur Rev Med Pharmacol Sci*. 2013;17:1233–1241.
93. Klabatsa A, Chicklore S, Barrington SF, Goh V, Lang-Lazdunski L, Cook GJ. The association of ^{18}F-FDG PET/CT parameters with survival in malignant pleural mesothelioma. *Eur J Nucl Med Mol Imaging*. 2014;41:276–282.
94. Flores RM, Akhurst T, Gonen M, et al. Positron emission tomography predicts survival in malignant pleural mesothelioma. *J Thorac Cardiovasc Surg*. 2006;132:763–768.
95. Gerbaudo VH, Mamede M, Trotman-Dickenson B, Hatabu H, Sugarbaker DJ. FDG PET/CT patterns of treatment failure of malignant pleural mesothelioma: relationship to histologic type, treatment algorithm, and survival. *Eur J Nucl Med Mol Imaging*. 2011;38:810–821.
96. Lee ST, Ghanem M, Herbertson RA, et al. Prognostic value of ^{18}F-FDG PET/CT in patients with malignant pleural mesothelioma. *Mol Imaging Biol*. 2009;11:473–479.
97. Lee HY, Hyun SH, Lee KS, et al. Volume-based parameter of ^{18}F-FDG PET/CT in malignant pleural mesothelioma: prediction of therapeutic response and prognostic implications. *Ann Surg Oncol*. 2010;17:2787–2794.
98. Marin-Oyaga VA, Salavati A, Houshmand S, et al. Feasibility and performance of an adaptive contrast-oriented FDG PET/CT quantification technique for global disease assessment of malignant pleural mesothelioma and a brief review of the literature. *Hell J Nucl Med*. 2015;18:11–18.
99. Ulaner GA, Lyall A. Identifying and distinguishing treatment effects and complications from malignancy at FDG PET/CT. *Radiographics*. 2013;33:1817–1834.
100. Ahmadzadehfar H, Palmedo H, Strunk H, Biersack HJ, Habibi E, Ezziddin S. False positive ^{18}F-FDG-PET/CT in a patient after talc pleurodesis. *Lung Cancer*. 2007;58:418–421.
101. Kwek BH, Aquino SL, Fischman AJ. Fluorodeoxyglucose positron emission tomography and CT after talc pleurodesis. *Chest*. 2004;125:2356–2360.
102. Peek H, van der Bruggen W, Limonard G. Pleural FDG uptake more than a decade after talc pleurodesis. *Case Rep Med*. 2009;2009:650864.
103. Niccoli-Asabella A, Notaristefano A, Rubini D, et al. ^{18}F-FDG PET/CT in suspected recurrences of epithelial malignant pleural mesothelioma in asbestos-fibers-exposed patients (comparison to standard diagnostic follow-up). *Clin Imaging*. 2013;37:1098–1103.
104. Nguyen NC, Tran I, Hueser CN, Oliver D, Farghaly HR, Osman MM. F-18 FDG PET/CT characterization of talc pleurodesis-induced pleural changes over time. *Clin Nucl Med*. 2009;34:886–890.
105. Vandemoortele T, laroumagne S, Roca E, et al. Positive FDG-PET/CT of the pleura twenty years after talc pleurodesis: three cases of benign talcoma. *Respiration*. 2014;87:243–248.
106. Fanggiday JC, Rouse RW, Collard SM, et al. Persistent inflammation in pulmonary granuloma 48 years after talcage pleurodesis, detected by FDG-PET/CT. *Case Rep Med*. 2012;2012:686153.
107. Li YJ, Zhang Y, Gao S, et al. Systemic disseminated tuberculosis mimicking malignancy on F-18 FDG PET-CT. *Clin Nucl Med*. 2008;33:49–51.
108. Yamamoto T, Seino Y, Fukumoto H, et al. Over-expression of facilitative glucose transporter genes in human cancer. *Biochem Biophys Res Commun*. 1990;170:223–230.